Influence of plasma nitriding on dry wear, corrosion and tribocorrosion performance of 17-4 precipitation hardening stainless steel

Auswirkungen des Plasmanitrierens von 17-4 ausscheidungsgehärteten Edelstahls auf Verschleiß, Korrosion und Tribokorrosionsverhalten

F. Mindivan[1], G.R. Aktas[2], A. Bayram[3]

Plasma nitriding treatment of 17-4 precipitation hardening stainless steels was carried out at 400 °C and 450 °C using a direct current unit. The nitriding layer thicknesses of the plasma nitrided at 400 °C and 450 °C were measured as 37.29 µm and 49.97 µm, respectively. The plasma nitrided sample at 400 °C presented dominant martensite and retained austenite phases; however, the height of main martensite diffraction peaks increased at 450 °C. The hardness results demonstrated that the samples at 400 °C and 450 °C were 2.9 and 3.1 times as hard as the untreated sample, respectively. The wear rate values of the sample at 450 °C showed a decrease by 19 % in the corrosive salt solution and 57 % in the dry-sliding condition compared with that of untreated sample. The corrosion potential of the sample at 400 °C had more positive potential value and lower current density value than those of at 450 °C. The corrosion resistance of the sample at 400 °C improved due to the positive effect of the retained austenite phase. In this study, the wear was more dominant rather than corrosion, therefore plasma nitrided sample at 450 °C showed the best dry wear and tribocorrosion resistance.

Keywords: 17-4 precipitation hardening stainless steel / plasma nitriding / dry-wear / corrosion / tribocorrosion

Schlüsselwörter: 17-4 ausscheidungsgehärteter Edelstahl / Plasmanitrieren / Verschleiß / Korrosion / Tribokorrosion

1 Introduction

The stainless-steel industry is a vital sector as it is a part of many different areas including the food, chemical, health, defense industry, automotive and marine construction. It also plays a key role in the manufacturing of power plant components. Although stainless steels are of attractive mechanical properties and corrosion resistance, their wear resistance and hardness are relatively low. 17-4 (american iron and steel institute 630) is a type of precipitation hardening stainless containing nearly

[1] Faculty of Engineering, Department of Bioengineering, Bilecik Seyh Edebali University, Bilecik, Turkey
[2] Tübitak- SAVTAG, Neighborhood of İşçi Blokları, Muhsin Yazıcıoğlu St., Ankara, Turkey
[3] Faculty of Engineering and Architecture, Department of Mechanical Engineering, Uludağ University, Görükle-Bursa, Turkey

Corresponding author: F. Mindivan, Faculty of Engineering, Department of Bioengineering, Bilecik Seyh Edebali University, Bilecik, Turkey,
E-Mail: ferda.mindivan@bilecik.edu.tr

3 % weight copper in its chemical composition. The precipitations of this copper are spread on to the matrix to greatly strengthen this steel [1, 2]. The 17-4 precipitation hardening stainless steel is a low carbon martensitic steel that is used in a wide range of industries due to high strength, excellent corrosion resistance, toughness, and good weldability [3]. 17-4 precipitation hardening stainless steel has been utilized in various areas of manufacturing including nuclear reactor components, aircraft fittings, chemical plants, gears, fasteners, in the petroleum chemical industry, compressor impeller, and oilfield components. However, low hardness and weak tribological properties of the 17-4 precipitation hardening stainless steel limits its areas of use [4–5]. The machine parts used functionally are subjected to many different forces while performing their function. There are many surface treatments applied to materials so that they can operate longer and their characteristics can be improved. The plasma nitriding process is a thermochemical surface hardening treatment that could improve the corrosion resistance, surface hardness, and wear properties of the samples. Plasma nitriding treatment is carried out at a temperature within the range of 350 °C to 590 °C by using gases such as ammonia, nitrogen, hydrogen, and argon. There are many different factors that affect the plasma nitriding process. The pressure, high voltage, and gas mixtures are crucial. In addition to these factors, the temperature and treatment time act on the properties of the nitrided part [6]. The reactions occurring during the plasma nitriding process are given below [7].

$$Fe + N = FeN$$

$$2FeN \rightarrow Fe_2N + N$$

$$3Fe_2N \rightarrow 2Fe_3N + N \ (\varepsilon\text{-phase})$$

$$4Fe_3N \rightarrow 3Fe_4N + N \ (\gamma'\text{-phase})$$

$$Fe_4N \rightarrow 4Fe + N$$

For example, it was reported that the plasma nitriding process improved wear resistance, hardness properties and pitting corrosion resistance of 17-4 precipitation hardening stainless steel [2, 8]. Surface properties and the transformations at the microstructure level played an important role in the decrease of wear rate of the 17-4 stainless steel samples after direct current plasma nitriding treatment at the temperature ranging from 350 °C to 480 °C for 4 hours [4]. The wear, corrosion and corrosion-wear behavior of plasma nitrided 17-4 precipitation hardening stainless steel was studied at the temperature ranging from 350 °C to 500 °C for 10 hours. It was also reported that the hardness, wear, corrosion and corrosion-wear behaviors of samples were dependent on the process conditions. Proper treatment conditions were found to improve the wear, corrosion, and corrosion-wear behaviors of the sample surface properties [9]. The structure and properties of american iron and steel institute 304 L steel after plasma nitriding at the temperatures ranging from 375 °C to 475 °C were investigated, and it was published that the plasma nitriding treatment resulted in a significant decrease in wear rate compared to untreated materials [10]. The wear resistance of american iron and steel institute 5140 steel were improved by means of plasma nitriding process parameters. The samples had maximum surface hardness and the best wear resistance. Therefore, it was suggested that the formation of a thin white layer and thick-high-hardness diffusion layer reduced wear loss of the material [11]. The wear and corrosion behaviors of plasma nitrided F53 super duplex stainless steel samples at the temperature of 350 °C–570 °C for 2 hours were studied. It was reported that the creation of different types of nitrides altered the hardness, wear and corrosion behaviour of the material [12]. The effects of low temperature plasma nitriding on the corrosion behavior and tribological properties of american iron and steel institute 420 stainless steel were investigated. The experimental studies were carried out with direct current-pulsed plasma nitriding unit in (1/3) 25 % nitrogen + 75 % hydrogen gas environment at 350 °C, 450 °C, 550 °C for 15 hours. It was further reported that the enhancement tribological properties of plasma nitrided 420 steels were obtained with the combination of good surface hardness, high compressive residual stress and the microstructure of the nitrided layer [13]. The tribological properties of plasma nitrided 316 stainless steel samples at the temperatures between 450 °C and 550 C° with a gas composition of 25 % nitrogen + 75 % hydrogen for 5 hours under pressure of 500 Pa were researched. It was reported that

the wear resistance and tribological properties of the plasma nitrided material changed with different types of phases and nitrided layer thickness and depended on the counterface material, the test parameters and treatment temperature values [14]. The plasma nitriding process was used to investigate wear resistance of a medical cast cobalt chrome molybdenum alloys. The treatment was carried out at different temperatures under a constant pressure of 500 Pa in a pure ammonia gas for 9 hours. The plasma nitriding process demonstrated positive effects on the wear behaviour. Eventually, good surface properties can be achieved with proper microstructure and a harder and thicker surface. Formed phases, microstructures, microhardness and distribution of microhardness of treated layers were discussed for all the samples [15]. Phase and microstructure of plasma nitrided 17-4 stainless steel were studied. Plasma nitriding treatment was carried out at the temperature between 350 °C–500 °C for 10 h to 30 h under a constant pressure of 500 Pa in a gas blend of 25 % nitrogen + 75 % hydrogen. The results showed that the microstructures and the phases of the plasma nitrided layers were highly dependant on plasma nitriding time and temperature [16]. This study is original in terms of two different dry wear tests and tribocorrosion tests on treated samples. The goal of this paper was to research and analyse the hardness, microstructure properties, dry wear, corrosion, and tribocorrosion behaviors of the plasma nitrided 17-4 precipitation hardening martensitic stainless steel under different plasma nitriding temperature conditions.

2 Material and method

2.1 Material and treatments

17-4 precipitation hardening martensitic stainless steel was chosen for experimental material in this study. The chemical composition of 17-4 precipitation hardening martensitic stainless steel was given, *Table 1*. The samples with a diameter of 25 mm and a height of 1 mm were used in this work. The planar faces were emeried with sand paper with the number of 180, 400, 600, 800, 1000. After grinding, these faces were polished by using 1 µm and 0.3 µm alumina paste for having smooth surfaces. A series of the experiment was carried out on 17-4 precipitation hardening stainless steel at the temperatures of 400 °C–450 °C using direct current plasma nitriding treatment modul in a 75 % nitrogen + 25 % hydrogen gas mixture at the pressure of 200 Pa for 12 hours [7].

2.2 Characterization

X-ray diffraction measurements were done by an x-ray diffractometer (PAN analytical, Empyrean) using a continuous scan mode to collect 2θ° from 10° to 90° (with a step size of 0.1°). Hardness values were obtained on the surface of untreated sample and the cross section of the plasma nitrided samples. Statical calculations were made and average hardness values were used. For obtaining the microstructure images, the untreated sample and plasma nitrided samples were polished using metallographic methods. Samples were etched for 60 seconds using a solution of hydrochloric acid (40 %) + nitric acid (20 %) + water (40 %). With the help of the Nikon LE150 optical microscope, the microstructures and the treated layer's surface morphologies were photographed at 200X and 500X magnifications. It was applied two different dry wear test for comperating the tribological properties. The literature was described different approaches for determining the friction properties [17]. The dry sliding tribological tests were performed at 13 rpm and 4 rpm. The dry sliding wear tests of the samples were measured using a ball-on-disc tribometer at a friction velocity 15 mm/s and 5 mm/s. A normal operating load of 1 kg and 0.7 kg was selected. Trace diameter was chosen 22 mm. Sampling frequency was 4 seconds. Tungsten carbide ball used as a counterface material. Wear loss was evaluated by the help of an ana-

Table 1. Chemical composition of 17-4 precipitation hardening stainless steel.

17-4 steel	C	Cr	Ni	Cu	Si	Mn	Nb	P	S	Mo	Ta
Composition (%)	0.021	15.72	4.73	3.28	0.31	0.71	0.30	0.02	0.001	0.16	0.004

lytical balance. The other dry wear tests were carried out on the samples using a reciprocating tribometer. An alumina ball with a diameter of 10 mm was used as counterpart. The wear tests were carried out at room temperature (24.5 °C), and at a relative humidity between 46 % and 54 % for all samples. All the tests were performed under a constant load of 0.5 kg (5 N) at a sliding velocity of 19 mm/s, < while sliding distance was 50 m. The alumina counterface surfaces were examined under an optical microscope and worn surface morphologies of samples were observed by using a Carl Zeiss AG, SUPRA 40 model field emission scanning electron microscopes. The friction coefficient was recorded using a computer during the wear test. The wear was calculated by analysing depth and width of wear scars developing on sample surfaces with the help of a contact stylus profilometer (SJ400). The electrochemical measurements were tested in 0.9 wt.% sodium chloride solution at room temperature via a Gamry model PCI4/750 potentiostat/galvanostat controlled by a computer with direct current 105 corrosion analysis software. Potentiodynamic polarization measurements were carried out with a potential scanning rate 1 $mV\,s^{-1}$ from catholic to anodic, starting from -1 V up to $+1$ V. The corrosion potential (E_{corr}) and corrosion current density (i_{corr}) were determined using the Tafel extrapolation method. The tribocorrosion tests of the untreated sample and plasma nitrided samples were made in a triboelectrochemical cell containing 25 ml of 0.9 wt.% sodium chloride solution by using a home-made tribometer with linear reciprocating system coupled with a three-electrode electrochemical cell. The tribocorrosion tests obtained in the three steps: (1) stabilisation of the open circuit potential for at least 10 min; (2) friction under the open circuit potential for 45 min; (3) stand by at the open circuit potential after friction for 10 min. The sliding started in a reciprocating system with 19 mm/s sliding velocity, normal load of 5 N and total sliding distance of 50 m. All corrosion and tribocorrosion tests were repeated at three times. Finally, the surface images of the corroded samples were examined using field emission scanning electron microscope, in order to determine the morphology of the developed corrosion and tribocorrosion.

3 Results and discussion

3.1 Microstructure analysis

The nitriding layer thickness of the plasma nitrided samples at 400 °C and 450 °C were measured as 37.29 µm and 49.97 µm, respectively. When the microstructures of the plasma nitrided samples at 400 °C and 450 °C were examined, two different regions which were diffusion layer and matrix were observed, *Figures 1, 2*. It is known that the matrix had martensite packets and copper atoms precipitate in the secondary hardened stainless steel [18, 19]. Generally, after plasma nitriding surface treatment, two layers are obtained to diffusion layer and white layer. Also, white layer called as compound layer. The white layer was not observed from optical microscope images of the plasma nitrided samples at 400 °C and 450 °C, *Figures 1*, *2*. The only diffusion layer was observed at a different thickness. Mechanical properties change depending on hardness, the treated layer's thickness and the formed phases. Especially, the mechanical characteristic of the material and its surface behaviour are

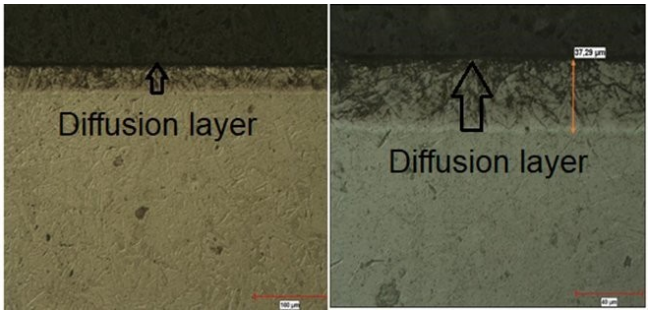

Figure 1. Optical microscope images of the plasma nitrided sample at 400 °C.

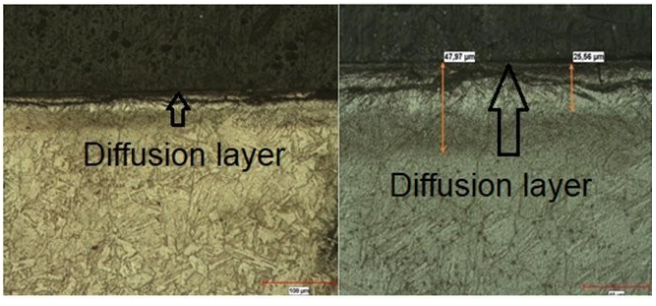

Figure 2. Optical microscope images of the plasma nitrided sample at 450 °C.

affected by the selected parameters. The structural properties of the compound layer and the diffusion layer are the most important factors affecting the properties of the plasma nitrided material [20]. The x-ray diffraction analysis results of this study gave clearer informations about the formed phases than that of optical microscope images. And it was explained the effect of these phases on the hardness, dry wear, corrosion and tribocorrosion properties of the plasma nitrided samples in other analysis sections.

3.2 X-ray diffraction analysis

Martensite (α) diffraction peaks were observed in the untreated sample, *Figure 3*. 17-4 stainless samples are generally dominated by martensite (α) phase peaks [16]. The plasma nitrided sample at 400 °C presented dominant martensite (α) and retained austenite (γ′-Fe_4N) phases, Figure 3. Retained austenite (γ‘-Fe_4N) has a face centred cubic organizing of iron atoms, which is widely knew to as ‘white layer’ because it seem white [9]. The optical microscope image of the plasma nitrided sample at 400 °C was not observed the white layer due to the low intensity of the peak of γ‘-Fe_4N in the surface regions, Figure 1. For plasma nitrided sample at 450 °C, the height of main martensite (α) diffraction peaks increased. The peaks of chromium nitride (CrN) were not observed in x-ray diffraction patterns of the plasma nitrided samples at 400 °C and 450 °C, Figure 3. It was described that can not be observed sharp Bragg reflection peaks at low-temperature (≤420 °C) and can be characterised by highly overlapped peaks as so-called ‘amorphous-like features’ [14]. Highly amorphous chromium nitride peaks at 460 °C were reported [16]. Sharp martensite (α) diffraction peaks probably overshadowed weak and amorphous chromium nitride peaks in this study. The crystalline size values of the martensite peak corresponding to 2θ° = 44.50° and 82.0° peaks decreased in the plasma nitrided sample at 400 °C in comparison to untreated sample, *Table 2*. But they remained the same in the plasma nitrided sample at 450 °C and untreated sample. The crystalline size values of the x-ray diffraction peak at 2θ° = 64.70°, 64.66° and 64.73°, corresponding to martensite (α) phase, increased

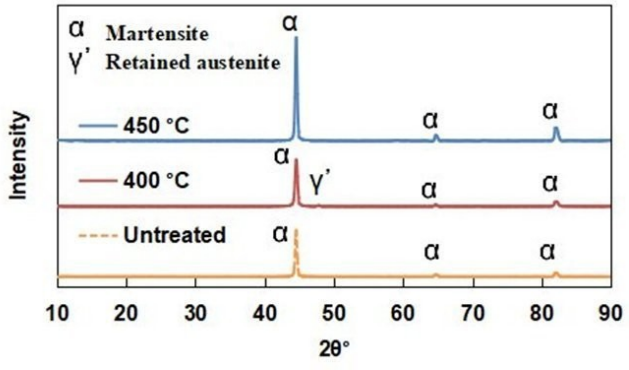

Figure 3. X-ray diffraction patterns of untreated sample and plasma nitrided samples.

Table 2. 2θ(°), crystallite size, and micro-strain values of untreated sample and plasma nitrided samples.

Sample	2 θ (°)	Crystallite size (Å)	Micro-strain (%)
Untreated	44.49	366.44	0.2778
	64.70	196.63	0.3663
	82.02	265.65	0.2211
400 °C	44.52	271.43	0.3748
	47.77	181.56	0.5242
	64.66	236.69	0.3045
	82.04	220.50	0.2663
450 °C	44.51	366.46	0.2777
	64.73	297.84	0.2417
	82.06	265.73	0.2209

with an increase of plasma nitriding temperature. The micro strain values changed depending on the increase and decrease in the crystalline size values inversely proportionally, Table 2.

3.3 Hardness analysis

The Vickers hardness test method was used for untreated sample and the plasma nitrided samples at 400 °C and 450 °C hardness measurements. Microhardness depth profile was carried out up to 400 µm from the surface. The average hardness of untreated sample was obtained 361.71 HV 1 which was in line with the observations by literature [14]. The hardness of the plasma nitrided samples at 400 °C and 450 °C were 1042.92 HV 0.025 and 1130.08 HV 0.025 at the 10 µm away from the surface, respectively. The plasma nitrided samples at 400 °C showed an abrupt decrease after a distance of 10 µm up to a distance of 40 µm, but the plasma nitrided samples at 450 °C showed a more gradual decrease. The highest hardness value and gradual microhardness decrease were obtained at the plasma nitrided sample at 450 °C, *Figure 4*. Plasma nitriding treatment was highly improved the surface hardness compared to untreated sample. The lower hardness result of the the plasma nitrided sample at 400 °C than the plasma nitrided sample at 450 °C was due to the retained austenite (γ'-Fe_4N) phase observed at $2\theta° = 47.77°$ determined by x-ray diffraction analysis, Figure 3. In addition, the higher hardness values of the plasma nitrided samples at 400 °C and 450 °C compared to the untreated sample were due to the increase in the the crystalline size values of the x-ray diffraction peaks corresponding to martensite (α) phase, Table 2.

3.4 Dry wear test by ball-on-disc tribometer

The wear tests were performed for untreated sample and the plasma nitrided samples at 400 °C and 450 °C on the dry sliding contidions. Pin-on-disc wear test applied. The loads were identified as 9.81 N (1 kg) and 6.867 N (0.7 kg) for this wear test. The Hertzian contact pressure for the load of 1 kg and 0.7 kg was respectively 1.9929 GPa and 1.773 GPa. The weight of all samples were evaluated before and after the wear test by the help of the analytical balance. The maximum wear loss was obtained by the plasma nitrided sample at 400 °C with 1 kg and a velocity of 15 mm/s, *Table 3*. And also, wear loss of untreated sample and the plasma nitrided sample at 400 °C were close to each other. When sliding velocity was high wear loss was also high. In other words, sliding velocity was caused to the increase of wear loss. In this study, the maximum wear loss occured at 1 kg load, Table 3. The plasma nitrided sample at 450 °C showed minimum wear loss. Plasma nitriding treatment made a good effect on wear resistance of the plasma nitrided sample at 450 °C. Scratch and microcracks were formed under the dry friction condition on untreated sample because of low surface hardness (361.71 HV 1), *Figures 5, 6*. Adhesive wear is a type of plastic deformation which results in superficial material debris creation. The friction between to the abrasive ball and the contact surface of the sample along the dry wear test produced the wear debris by the way of fracture. Both abrasive and also adhesive wear was occurred on the untreated sample, Figures 5, 6. Thin scratches were seen in certain regions. It was observed from the wear weight loss of untreated sample that wear debris increased with the increased of

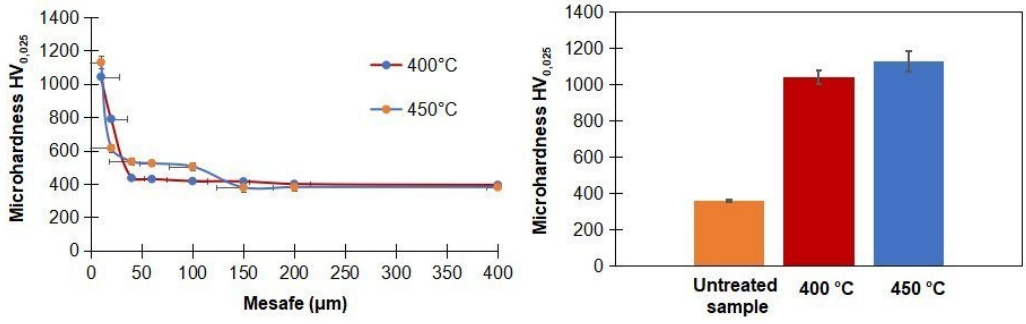

Figure 4. Microhardness depth profile and results of untreated sample and plasma nitrided samples.

Table 3. Sample weights before and after the dry sliding wear test.

Wear loss (g)		15 mm/s		5 mm/s	
		1 kg	0.7 kg	1 kg	0,7 kg
Untreated sample	Initial	48.2801	49.0394	47.6539	49.7877
	Final	48.2743	49.0353	47.6526	49.7866
	Difference	0.0058	0.0041	0.0013	0.0011
400 °C	Initial	50.3878	49.4987	47.3657	48.2801
	Final	50.3816	49.4932	47.3630	48.2785
	Difference	0.0062	0.0055	0.0027	0.0016
450 °C	Initial	49.6439	49.1912	48.5508	48.1296
	Final	49.6401	49.1880	48.5506	48.1294
	Difference	0.0038	0.0032	0.0002	0.0002

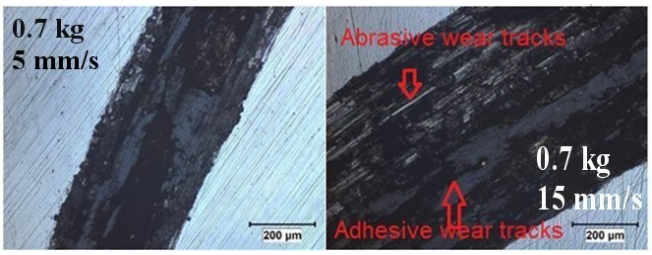

Figure 5. Optical microscope images of untreated sample at the 0.7 kg load, 5 and 15 mm/s sliding velocity by ball-on-disc tribometer.

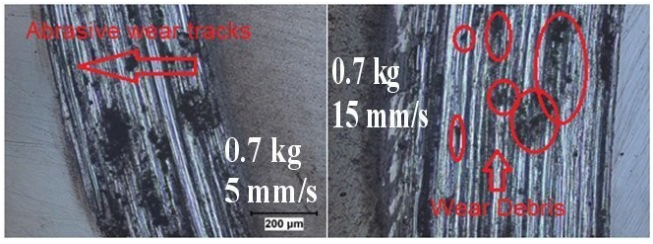

Figure 7. Optical microscope images of the plasma nitrided sample at 400 °C at the 0.7 kg load, 5 and 15 mm/s sliding velocity by ball-on-disc tribometer.

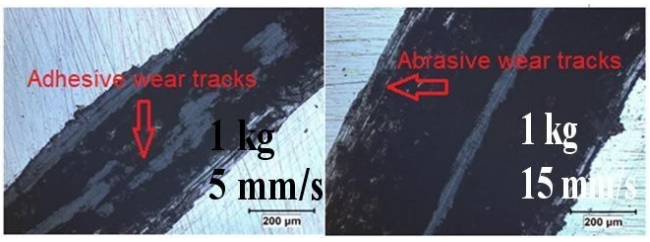

Figure 6. Optical microscope images of untreated sample at the 1 kg load, 5 and 15 mm/s sliding velocity by ball-on-disc tribometer.

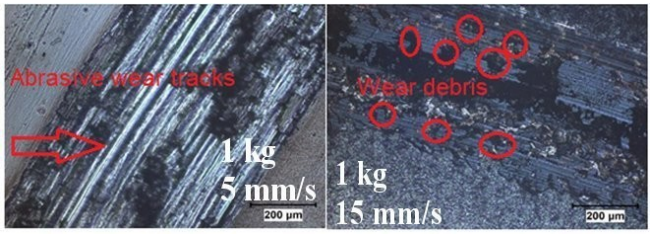

Figure 8. Optical microscope images of the plasma nitrided sample at 400 °C at the 1 kg load, 5 and 15 mm/s sliding velocity by ball-on-disc tribometer.

sliding distance, Table 3. The abrasive particles between the sample and the counterface ball increased abrasive wear for the plasma nitrided sample at 400 °C, *Figures 7, 8*. Because of this reason, deformation and wear loss was also high. The plasma nitrided sample at 400 °C had principally abrasive wear. Plastic deformation and scratches occurred and wear loss was also relatively high, Table 3. When the sliding velocity or sliding distance increased, the deeper starches were observed, Figures 7, 8. The optical microscope images of the plasma nitrided sample at 450 °C indicated superficial scratches, *Figures 9*, *10*. The plasma nitrided sample at 450 °C exhibited the best wear resistance in comparison to other samples. Wear loss was quite low in comparison to the plasma nitrided sample at 400 °C and untreated sample, Table 3. There were microcracks and scratching on the plas-

Figure 9. Optical microscope images of the plasma nitrided sample at 450 °C at the 0.7 kg load, 5 and 15 mm/s sliding velocity by ball-on-disc tribometer.

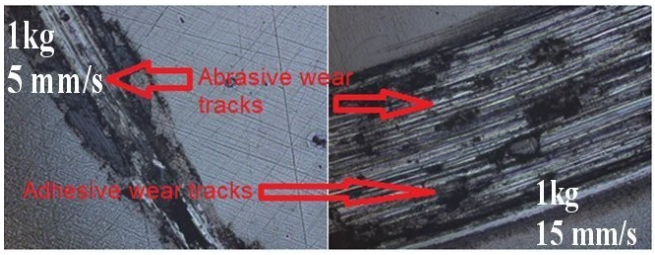

Figure 10. Optical microscope images of the plasma nitrided sample at 450 °C at the 1 kg load, 5 and 15 mm/s sliding velocity by ball-on-disc tribometer.

ma nitrided sample at 450 °C, but it was minimal in comparison to the plasma nitrided sample at 400 °C and untreated sample. Deep scratches were observed with the increasing of sliding velocity and loading amounts for the plasma nitrided sample at 450 °C. The sliding wear resistance of the nitrided material was evaluated using a pin-on-disc tribometer sliding against a tungsten carbide ball by the study [9]. It was observed similiar images with this study and reported that 17-4 precipitation hardening sample abrasive and adhesive wear tracks as evidenced by grooves and adhesive craters, respectively. After plasma nitriding, the wear tracks were shallow, superficial and very smooth on a macroscale. On a microscale, adhesion and plastic deformation with deep abrasive grooves were occured. Untreated sample showed the highest coefficient of friction variation in all conditions except 0.7 kg load and 5 mm/s condition, *Figure 11*. Although it started with a higher friction coefficient than both nitrided samples at the beginning, it showed friction behavior below the plasma nitrided sample at 400 °C in the first 20 meters sliding distance and also below the plasma nitrided sample at 450 °C in the last 20 meters sliding distance at 0.7 kg load and 5 mm/s condition. In addition, the plasma nitrided sample at 400 and 450 samples represented similar friction coefficient changes in the last 20 meters sliding distance, Figure 11. This result was due to the absence of abrasive wear tracks in the optical microscope image of the untreated sample, and its all-wear surface had adhesive wear tracks. Abrasive wear tracks were clearly visible at the plasma nitrided samples at 400 °C and 450 °C,

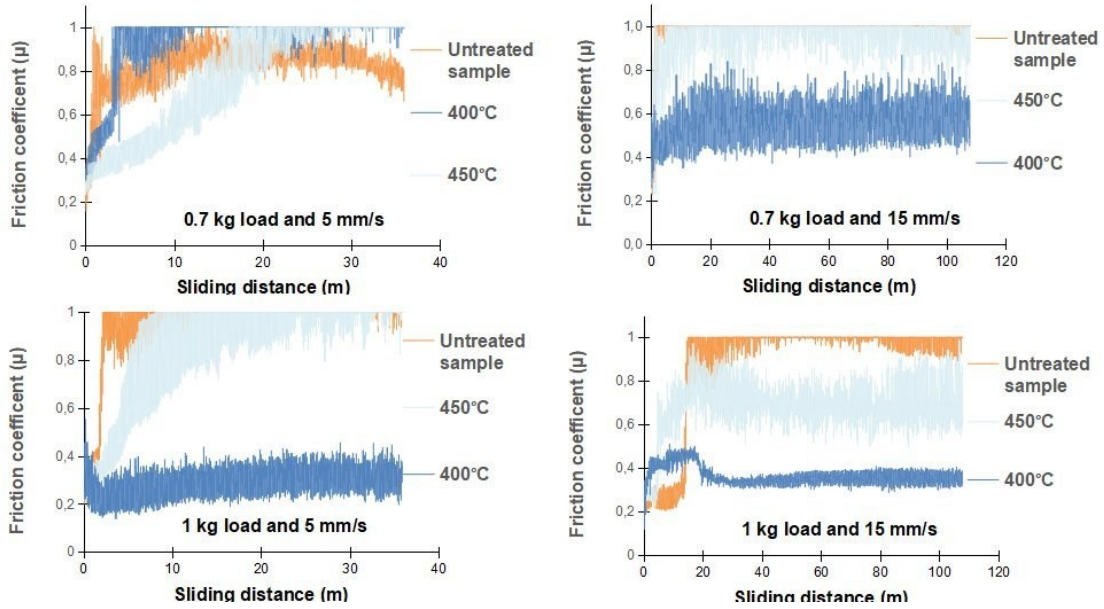

Figure 11. Friction curves of untreated sample and plasma nitrided samples obtained with a ball-on-disc tribometer.

Figures 7, 9. In other conditions, the plasma nitrided sample at 400 °C had the lowest friction coefficient variation with more adhesive wear tracks. In addition, when the sliding speed values were kept constant, it was determined that the friction coefficient of nitrided samples decreased with the increased of load.

3.5 Dry wear test by reciprocating tribometer

The stable friction coefficients of the untreated sample and the plasma nitrided sample at 400 °C were found to be similar (1.27 ± 0.2 for the untreated sample, 1.29 ± 0.1 for the plasma nitrided sample at 400 °C), *Figure 12*. However, the sliding curves of the untreated sample exhibited larger fluctuation than the plasma nitrided sample at 400 °C. This large fluctuation in the sliding curves resulted from the lower surface hardness of the untreated sample. The friction coefficient values of the reciprocating wear test results that performed at a lower load (0.5 kg) but at a higher speed (19 mm/s) were compatible with the ball on disc wear tests results. The friction coefficient value of the plasma nitrided sample at 450 °C at 0.5 kg and 19 mm/s was 1.12 ± 0.5 but same sample had friction coefficent values 0.9 ± 0.3 at 0.7 kg at 15 mm/s and 0.7 ± 0.1 at 1 kg at 15 mm/s, Figures 11, 12. This result showed that the friction coefficient decreased with the increased loading in both wear test results at almost close sliding velocity. The lowest friction coefficient value was obtained for the plasma nitrided sample at 450 °C, Figure 12. The plasma nitrided sample at 450 °C had the lowest wear volume and wear rate than those of samples, *Table 4*. Comparing with untreated sample and the plasma nitrided sample at 400 °C, the plasma nitrided sample at 450 °C possessed both the best friction-reducing ability and wear resistance. According to the wear rates, it was quantified that wear resistance of the plasma nitrided sample at 450 °C was 57.44 times higher than that of the untreated sample. It was reported that dry-sliding wear resistance decreases with increasing formation of chromium nitrides and chromium iron oxide but was claimed that excellent wear resistance can be provided with the formation of a small quantity of chromium iron oxide [15]. In this study, the peaks of chromium nitride (CrN) were not observed in x-ray diffraction patterns of the plasma nitrided samples at 400 °C and 450 °C but as described in the x-ray diffraction analysis section intense martensite (α) diffraction peaks probably covered up weak and amorphous chromium nitride peaks in this study, Figure 3. Chromium nitride was probably formed at the plasma nitrided sample at 450 °C. The presence of retained austenite at the x-ray diffraction pattern of the plasma nitrided sample at 400 °C could be shown as the reason of the decrease in wear resistance. Because the expanded (γ_N) and retained (γ') austenite peaks were not available at 450 °C. In this temperature, the formation of mixed layer of martensite (α) phase and chromium nitride was favoried in the example ($\gamma_N \rightarrow \alpha + CrN$) and martensite (α) predominated in this mixed layer. Therefore, the formation of some amount chromium nitride increased the wear resistance at the plasma nitrided sample at 450 °C.

The wear width of untreated sample and the plasma nitrided sample at 400 °C got big than that of the plasma nitrided sample at 450 °C, *Figure 13*. From the high magnification images of the untreated sample and the plasma nitrided sample at

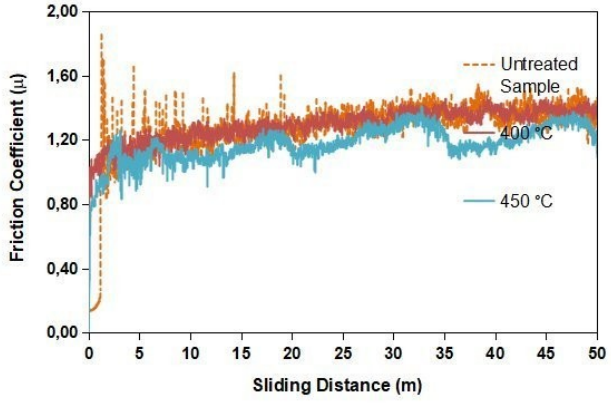

Figure 12. Friction curves of untreated sample and plasma nitrided samples obtained with a reciprocating tribometer.

Table 4. Wear volumes and wear rates of samples under dry sliding condition.

Samples	Wear volumes (mm^3)	Wear rates (mm^3/Nm)
Untreated	0.1983	3.9×10^{-4}
400 °C	0.2700	5.4×10^{-4}
450 °C	0.0834	1.66×10^{-4}

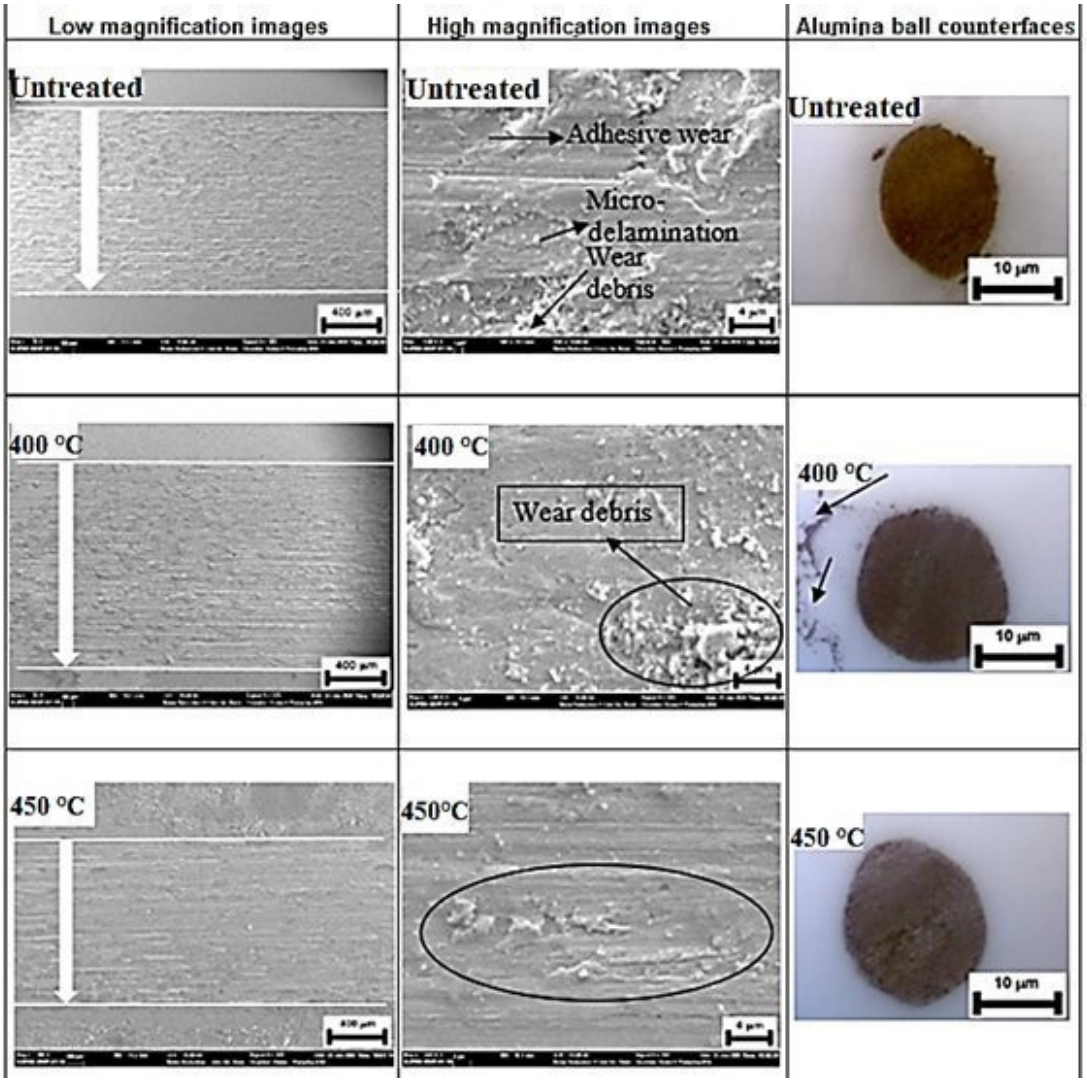

Figure 13. Field emission scanning electron microscope images of worn surfaces and the alumina ball counterfaces of samples obtained with a reciprocating tribometer.

400 °C, it can be seen that the severe adhesive wear by plastic deformation tracks were found dominant. On the other hand, micro-delamination was evident in the surface images, because a large number of fragments of surface were produced during the severe wear process, Figure 13. The wear resistance of 17-4 precipitation hardening stainless steel was investigated and reported that the wear mechanisms of 17-4 stainless steel was micro-grooving, adhesion and micro-delamination [21]. It was expected to be much lower friction coefficient, wear volume and wear rate values of the plasma nitrided sample at 400 °C than the untreated sample. Due to wear debrises acted as a second body, the plasma nitrided sample at 400 °C exhibited the lowest wear resistance. In order to explain this unexpected result, the alumina ball counterfaces were analysisd by optical microscope. The worn surface morphology of alumina ball against untreated sample was similar to that of the plasma nitrided sample at 400 °C and they have rather dense transfer film on the alumina balls but also the transferred debris was obseved outside the center of the alumina ball that contacted with the plasma nitrided sample at 400 °C, Figure 13. This image of counterface was consistent with the results obtained from friction coefficient, wear rate and wear volume of the plasma nitrided sample at 400 °C, Figure 12, Table 4. The wear tracks of the plasma nitrided sample at 450 °C depicted less and smaller wear debris as

compared to the untreated sample and the plasma nitrided sample at 400 °C and adhesive, micro-delamination wear tracks decreased on a large scale, Figure 13. Wear tracks of the plasma nitrided sample at 450 °C showed formation of thin and uniform a transfer layer on the alumina ball surface.

3.6 Potentiodynamic corrosion tests

The current density (I_{corr}) value of the plasma nitrided sample at 450 °C was higher than that of untreated sample and the plasma nitrided sample at 400 °C but current density values of untreated sample and the plasma nitrided sample at 400 °C were quite similar, and the corrosion potential (E_{corr}) values of the plasma nitrided samples were more negative than that of untreated sample, *Figure 14*, *Table 5*. The untreated sample showed the best resistance to corrosion in 0.9 wt. % sodium chloride solution, Figure 14. The corrosion potential of the plasma nitrided sample at 400 °C had more positive potential value (−244 mV) and lower current density value (0.515 A/cm^2) than those of the plasma nitrided sample at 450 °C (−422 mV and 14.3 A/cm^2).

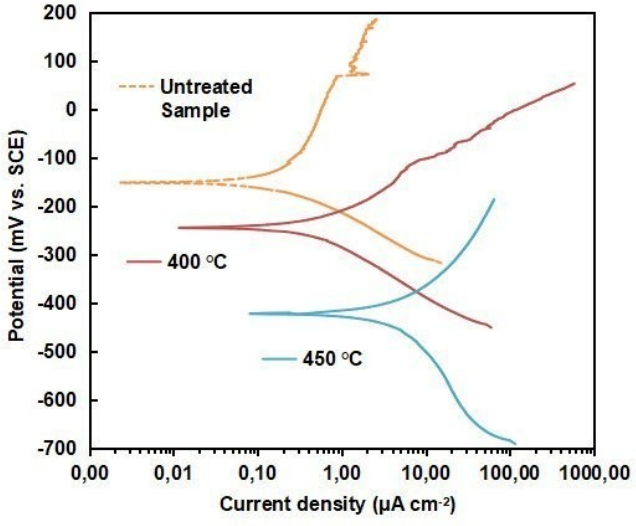

Figure 14. Tafel polarisation curves of untreated sample and plasma nitrided samples 0.9 wt.% sodium chloride solution.

Table 5. Corrosion data obtained from Tafel polarisation tests of untreated sample and plasma nitrided samples in 0.9 wt.% sodium chloride.

	Untreated	400 °C	450 °C
Corrosion potential (mV)	−151	−244	−422
Current density (A/cm^2) × 10^{-6}	0.434	0.515	14.3

Similar corrosion results with this study were reported by literature [2]. 17-4 precipitation hardening stainless steel was plasma nitrided at 400 °C for 5 and 10 hours, 450 °C for 5 hours and 500 °C for 5 hours. The corrosion potential of samples nitrided at 400 °C is more noble than that of those nitrided at 450 °C and 500 °C. This result to the formation of passive oxide film on the surface was attributed since the chromium remained in the matrix at this temperature [2]. But a protective passive layer did not form due to chromium nitrides could form at 450 °C and 500 °C and the amount of chromium could reduce in solid solution. The positive effect of retained austenite (γ'-Fe_4N) phase in improving the corrosion resistance of treated 17-4 stainless steel was explained by other study [9]. In another study, it was reported that the reduction of the diffusion of chromium and the formation of chromium-rich precipitates, the formation of the martensite can improve corrosion resistance [22]. The presence of retained (γ') austenite phase peak at the x-ray diffraction pattern of the plasma nitrided sample at 400 °C could be shown as the reason of the increase in corrosion resistance, Figure 3.

The low and high magnification field emission scanning electron microscope images of untreated and plasma nitrided samples after Tafel polarisation test in 0.9 wt.% sodium chloride, *Figure 15*. The plasma nitrided sample surfaces seemed less damaged in low magnification field emission scanning electron microscope images. On the other hand, on the untreated sample surface, there was signatures of corrosion attack, and shallow pits. In the high magnification field emission scanning electron microscope images of samples, the plasma nitrided samples had deep corrosion pits that unevenly distributed in the whole surface. These deep pits caused to reduce of corrosion resistances at the plasma nitrided samples. The field emission scanning electron microscope images indicated that local corrosion occurred at plasma nitrided samples. And also, the corrosion surfaces of the plasma nitrided samples appeared quite different, Figure 15. The surface of the plasma nitrided sample at 450 °C

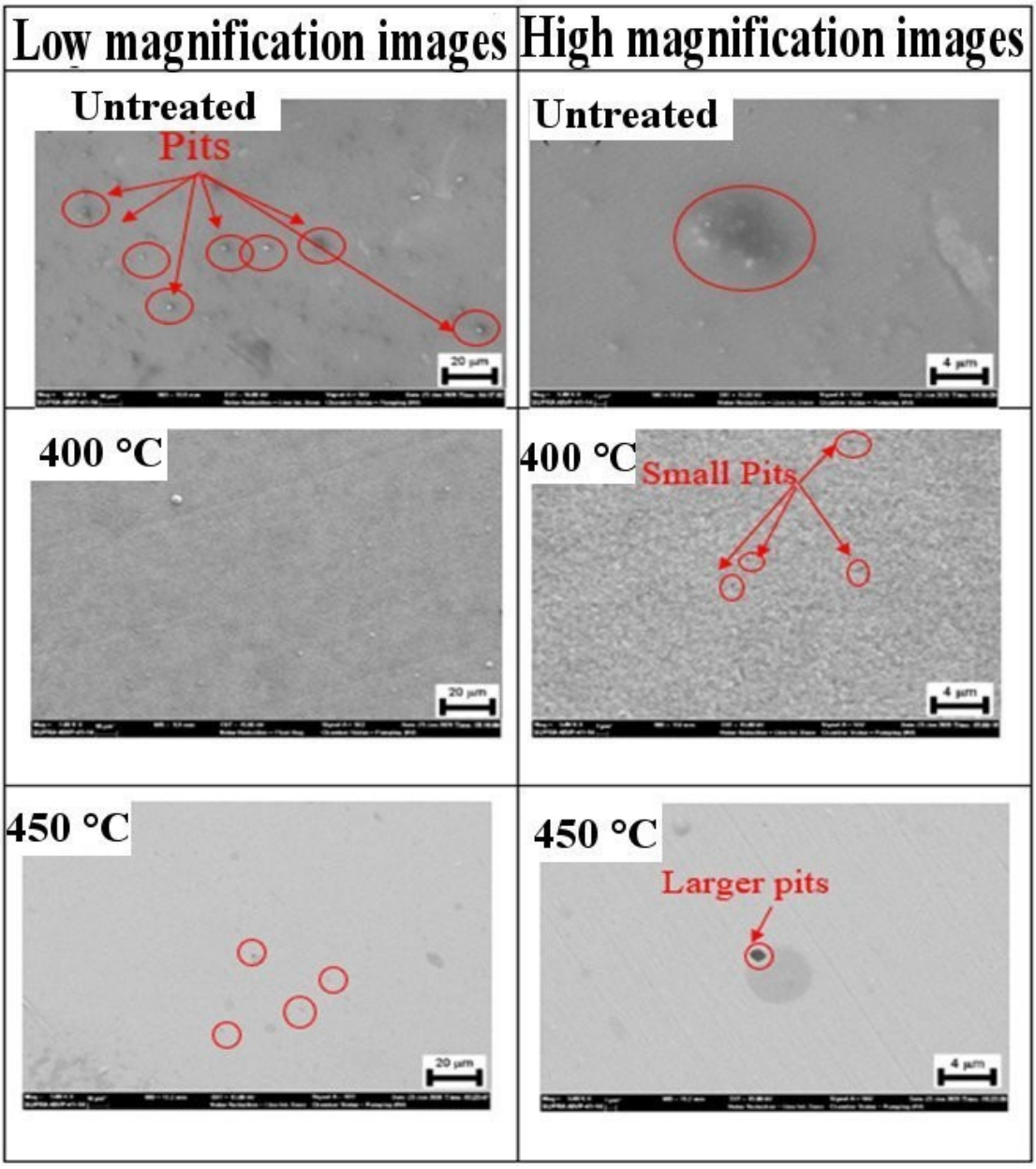

Figure 15. Low and high magnification field emission scanning electron microscope images of untreated sample and plasma nitrided samples after Tafel polarisation test in 0.9 wt.% sodium chloride.

was smoother, while the surface of the plasma nitrided sample at 400 °C looked rougher. In addition, there were very small pits in the plasma nitrided sample at 400 °C but were observed in the plasma nitrided sample at 450 °C. This difference between the surfaces affected the corrosion resistances of plasma nitrided samples and it was presented similar images in the literature [2]. They observed very small diameter pits at 400 °C. In contrast their samples had fewer but higher average diameter at 450 °C and 500 °C. In these temperatures, growth of the nucleated pits increases because nitrogen atoms bonded with chromium and iron to make their nitrides and lack of free nitrogen atoms cause lack of ammonia and ammonium formation in the solution.

3.7 Tribocorrosion test

Before starting of the sliding, open circuit potential of untreated sample was higher than the plasma nitrided samples, *Figure 16*. But, when sliding started, a very higher drop in the potential of untreated sample was observed than plasma nitrided samples. Both plasma nitrided samples had a small drop. The sudden drop of open circuit potential indicated a partial removal of the passive film. And it was understood that more stable passivation layer formed on the surface of plasma nitrided samples owing to the nitriding treatment. The synergistic effect of wear and corrosion action caused an increase in susceptibility of the untreated sample, and therefore a need for surface protection. When sliding started, it can be clearly seen that the plasma nitrided samples always presented relatively higher potentials and indicating a lower tendency to corrosion and wear than untreated sample, Figure 16. Once the sliding motion stopped, the open circuit potential of all samples did not recover the initial value, the plasma nitrided samples showed similar increases, but untreated exhibited a little more increase due to passivation of active surfaces with oxidation. Besides, the corresponding high friction coefficient value and its fluctuations for the untreated sample provided supplemental evidence for the open circuit potential variations. Plasma nitrided samples had lower and more stable friction coefficent values compared to untreated sample, *Figure 17*.

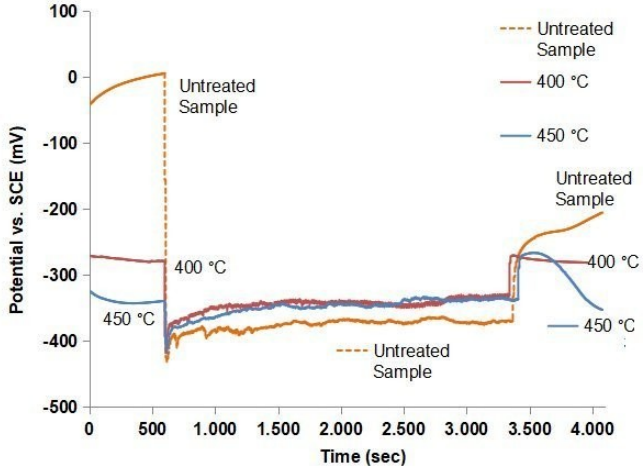

Figure 16. Variation of the potential during the open circuit potential tribocorrosion tests.

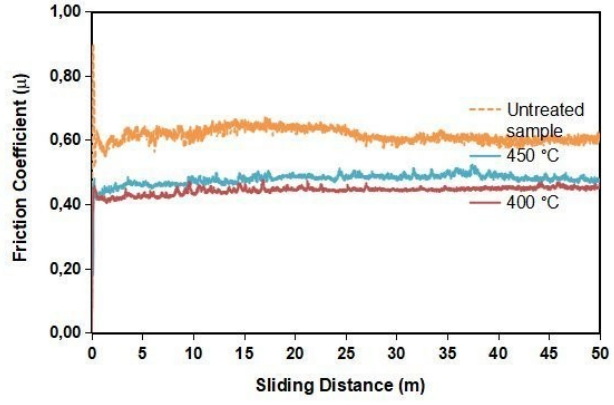

Figure 17. Variation of friction coefficient during the open circuit potential tribocorrosion tests.

The wear volume and rate values of the plasma nitrided sample at 400 °C increased both tribocorrosion and dry wear conditions Tables 4, *6*. This result was attributed that retained austenite (γ'-Fe_4N) with surface layer of the plasma nitrided sample at 400 °C removed by mechanical rubbing led to poor dry wear resistance and poor tribocorrosion resistance [9]. But the wear rate of the plasma nitrided sample at 450 °C decreased by 19 % in the corrosive salt solution and 57 % in the dry wear environment compared with that of untreated sample, Tables 4, 6. Less reduction in wear rate was an expected result due to corrosive solution. It was determined that the plasma nitrided sample at 450 °C was resistant to dry wear condition, but the plasma nitrided sample at 400 °C was more robust to corrosion. And also, in the tribocorrosion test, it was understood that wear was more dominant rather than corrosion, because the plasma nitrided sample at 450 °C showed the best result. Characterization of the worn samples using field emission scanning electron microscope revealed that the untreated sample /alumina ball contact yielded deep grooves in the wear track along the sliding direction as well

Table 6. Wear volumes and wear rates of samples after the open circuit potential tribocorrosion tests.

Samples	Wear volumes (mm^3)	Wear rates (mm^3/Nm)
Untreated	0.0105	0.21×10^{-4}
400 °C	0.0121	0.24×10^{-4}
450 °C	0.0089	0.17×10^{-4}

as pores due to the corrosion tests, *Figure 18*. On the contrary, the plasma nitrided sample at 400 °C and the plasma nitrided sample at 450 °C alumina ball contact yielded a smooth morphology slightly affected by the tribological contact. However, there were more pits on the surfaces of the plasma nitrided samples at 400 °C and 450 °C compared to untreated sample. The same size pits were seen in the plasma nitrided sample at 400 °C, but big and little mixed pits were appeared in the plasma ni-

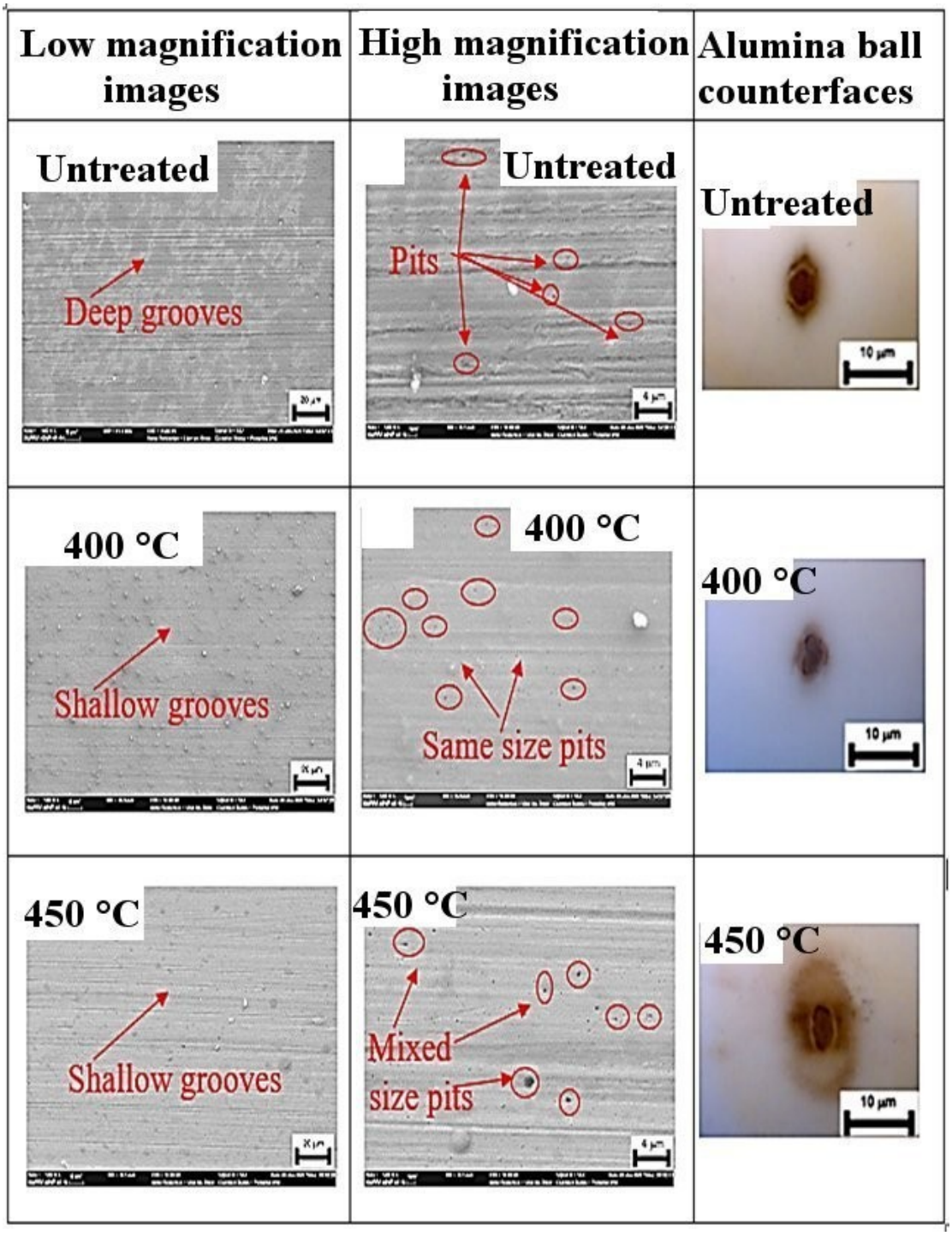

Figure 18. Worn surface field emission scanning electron microscope micrographs of untreated sample and plasma nitrided samples after tribocorrosion tests.

trided sample at 450 °C, Figure 18. This result confirmed the corrosion results again. The untreated sample showed the best resistance to corrosion than the plasma nitrided samples in the corrosion test and presented less porous images after corrosion and tribocorrosion tests.

4 Conclusion

In this study, plasma nitriding process was applied at the temperatures of 400 °C and 450 °C for 12 hours at the steady pressure 200 Pa condition and in a gas combination of 75 % nitrogen + 25 % hydrogen gas on 17-4 precipitation hardening stainless steel. The microstructure, dry wear, corrosion and tribocorrosion behaviours of plasma nitrided samples were examined. According to the results and discussion sections, the conclusions obtained from this research were given below.

- According to optical microscope images and x-ray diffraction analysis results, martensite (α) phase dominated at untreated sample but the plasma nitrided sample at 400 °C had martensite (α) and retained austenite (γ′-Fe_4N) phases. And thickness of the treated layer enhanced from 37.29 µm for the plasma nitrided sample at 400 °C to 47.97 µm for the plasma nitrided sample at 450 °C.
- The plasma nitriding treatment improved the microhardness of the plasma nitrided samples. The maximum hardness value obtained the plasma nitrided sample at 450 °C average 1130 HV 0.025. The crystalline size value of the x-ray diffraction peaks corresponding to martensite (α) phase, increased with an increase of plasma nitriding temperature and supported the rise in both α phase and microhardness value at the plasma nitrided sample at 450 °C.
- Wear rate of untreated sample, the plasma nitrided samples at 400 °C and 450 °C increased with the sliding velocity at pin-on-disc wear test. Wear behaviour of the untreated sample was poor due to having low hardness. After the plasma nitriding treatment, dry sliding wear behaviour of the plasma nitrided sample at 450 °C had the best wear resistance. The maximum amount of wear loss was seen in the plasma nitrided sample at 400 °C. Minimal microcracks and scratching were observed on the plasma nitrided sample at 450 °C, but abrasive-adhesive wear tracks were present at the plasma nitrided sample at 400 °C and untreated sample and the deep starches were observed at the same samples when the sliding velocity or sliding distance increased.
- The other dry wear test results (reciprocating test) showed that the plasma nitrided sample at 450 °C possessed the lowest friction coefficient value, wear volume and wear rate than those of samples. The wear resistance of the plasma nitrided sample at 450 °C was 57.44 times higher than that of the untreated sample.
- The decrease in wear resistance of the plasma nitrided sample at 400 °C attributed to the presence of the retained (γ′) austenite phase. A small quantity of chromium nitride (CrN) at the plasma nitrided sample at 450 °C caused the best friction-reducing ability and wear resistance. The severe adhesive wear by plastic deformation was evident on the surface images of the untreated sample and the plasma nitrided sample at 400 °C. But the adhesive and micro-delamination wear tracks decreased on a large scale at the plasma nitrided sample at 450 °C.
- The formation of passive oxide film on the plasma nitrided sample at 400 °C surface due to the presence of retained (γ′) austenite phase caused the plasma nitrided sample at 400 °C had more positive potential and lower current density values than those of the plasma nitrided sample at 450 °C.
- The plasma nitrided sample at 400 °C had both poor dry wear resistance and tribocorrosion resistance but the plasma nitrided sample at 450 °C showed decrease by 19 % in the corrosive salt solution and 57 % in the dry wear environment compared with that of untreated sample. Under open circuit potential conditions, the plasma nitrided sample at 450 °C exhibited better tribocorrosion performance when compared to the untreated and the plasma nitrided sample at 400 °C. This was attributed to their improved high hardness and therefore high resistance to wear.

Acknowledgements

We would like to express our thanks to Dr Ersin. E. KORKMAZ (Er-Mir Tekstil ve Makina San. Tic.

Ltd.Şti., Bursa, Turkey) for the support given in nitriding process.

5 References

[1] E. Menthe, K.T. Rie, J.W. Schultze, S. Simson, *Coat. Technol.* **1995**, *74–75*, 412.
[2] H. Riazi, F. Ashrafizadeh, A. Eslami, *Can. Metall. Q.* **2017**, *56 (3)*, 322.
[3] N.S. Mahesha, R. Hanumantharaya, B.D. Mahesh, D.P. Ramakrishna, K.M. Shivakumar, *Am. J. Mater. Sci.* **2016**, *6 (4A)*, 6.
[4] G-j. Li, J. Wang, C. Li, Q. Peng, J. Gao, B-l. Shen, *Nucl. Instrum. Methods Phys. Res. B* **2008**, *266 (9)*, 1964.
[5] M.S. Della Roverys Coseglio, *Mater. Sci. Technol.* **2017**, *33 (16)*, 1863.
[6] D. Kovács, A. Kemény, J. Dobránszky, I. Quintana, *Iop. Conf. Ser. Mater. Sci. Eng.* **2018**, *426*, 012027.
[7] G.Ö. Aktaş, *Msc. Thesis* Bursa Uludağ University, Turkey, **2019**.
[8] M.S. Della Roverys Coseglio, X. Li, H. Dong, B.J. Connolly, P. Dent, C. Fowler, *Corrosion* **2019**, *75(10)*, 1237.
[9] M. Esfandiari, H. Dong, *Surf. Coat. Technol.* **2007**, *202 (3)*, 466.
[10] E. Menthe, K.T. Rie, *Surf. Coat. Technol.* **1999**, *116–119*, 199.
[11] S. Karaoğlu, S. Karadeniz, C. Karaoğlu, *DEU FMD.* **2001**, *3 (3)*, 85.
[12] J.O.P. Neto, R.O. Silva, E.H. Silva, J.A. Moreto, R.M. Bandeira, M.D. Manfrinato, L.S. Rossino, *Mater. Res.* **2016**,*19 (6)*, 1241.
[13] Y.T. Xi, D.X. Liu, D. Han, *Surf. Coat. Technol.* **2008**, *202 (12)*, 2577.
[14] Y. Sun, T. Bell, *Wear* **1998**, *218 (1)*, 34.
[15] J. Wang, Y. Lin, H. Fan, D. Zeng, Q. Peng, B. Shen, *JMEPEG* **2012**, *21*, 1708.
[16] H. Dong, M. Esfandiari, X.Y. Li, *Surf. Coat. Technol.* **2008**, *202 (13)*, 2969.
[17] J.L. do Vale, C.H. da Silva, G. Pintaude, *Ind. Lubr. Tribol.* **2020**, *72(9)*, 1103–1108.
[18] P. Kochmanski, J. Nowacki, *Surf. Coat. Technol.* **2008**, *202 (19)*, 4834.
[19] M. Murayama, K. Hono, Y. Katayama, *Metall. Mater. Trans. A.* **2007**, *30 (2)*, 345.
[20] S.Y. Güven, K. Delikanlı, E. Öncel, *SDU J. Tech. Sci.* **2014**, *4 (2)*, 29.
[21] J.D. Bressan, D.P. Daros, A. Sokolowski, R.A. Mesquita, C.A. Barbosa, *J. Mater. Process. Technol.* **2008**, *205*, 355.
[22] E.A. Bernardelli, P.C. Borges, L.C. Fontana, J.B. Floriano, *Kovove Mater.* **2010**, *48* (2), 1.

Received in final form: May 10th 2022